Comparing SiC MOSFET, IGBT and Si MOSFET in LV distribution inverters

N.M. Roscoe*, Y. Zhong, S.J. Finney
Department of Electronic and Electrical Engineering
University of Strathclyde, Glasgow, UK
* nina.roscoe@strath.ac.uk

***Abstract*—Efficency, power quality and EMI are three crucial performance drivers in LVDC applications such as electrical supply, EV charging or DC aerospace. Recent developments in SiC MOSFETs and MMC for LVDC promise two significant improvements in LVDC inverter performance. However, the designer is left with many combinations of technology and inverter level to choose from. This paper aims to clarify this choice by identifying one optimum Si design and one optimum SiC design, using detailed loss calculations. An IGBT inverter is included as a baseline. Loss calculations estimate the effects of Si MOSFET switching loss and all parasitic interconnection loss. The validity of the loss estimations are verified using careful experiments on a Si MOSFET cell. Close agreement indicates that the modelling approach is valid for extension to many cells in series, and to the parallel connection of many devices. Despite the lower EMI inherent in MMC inverters, Si MOSFETs risk worse EMI, due to poor reverse recovery characteristic. Slowed device gate switching experimentally demonstrates the reduction in switching noise, promising very low EMI. This initial study has therefore identified two promising candidate SiC and Si MOSFET inverters which will be fully constructed in future work, in order to aid designers in choosing the optimum semiconductor technology and topology for LVDC inverters.**

Keywords—Si MOSFET; MMC; SiC MOSFET; loss calculation; efficiency; EMI; EMC; ringing; voltage overshoot; diode reverse recovery; power quality

I. INTRODUCTION

DC-AC converters with high efficiency and high power quality are in increasing demand. Switching to a low voltage dc (LVDC) distribution system simplifies a utility network, leading to improved reliability, elimination of frequency stability and skin effect issues, and improved control over power factor at the point of use [1,2]. Drivers for utility networks include low volume, high power quality, very high efficiency and longevity, and demanding targets for distribution system losses must be met. DC aerospace systems constitute a further LVDC application, where volume and weight are critical (making thermal management highly challenging) and strict EMI requirements must be met, while constantly improving performance and reducing fuel consumption.

To summarize, realizing the advantages of LVDC therefore requires development of highly efficient, high power quality, low EMI inverters. Modular multilevel converters (MMC) have traditionally only been used at HV and MV, however recent work has suggested that when Si MOSFET MMC are applied to LV inverters [2,3], efficiency is improved compared with 2-level inverters. However, the increasing availability of SiC complicates the choice of circuit topology for an LV inverter. It is not currently clear whether SiC or Si MOSFETs will offer superior performance in LVDC applications. This work uses highly detailed theoretical analysis to present an initial comparison of semiconductor technologies for LVDC. Using these results, the myriad possible combinations of semiconductor technology and inverter topology can be reduced to just two circuits which can be compared in full scale experiments to compare SiC and Si MOSFETs for LVDC. Analysis includes all parasitic interconnection losses incurred in the parallel combination of devices, and in the series connection of cells to create MMC. These losses are added in the form of series resistance to the on-state resistance exhibited by the devices. The accuracy of predictions for interconnection loss is experimentally verified using a single MMC cell. This loss, which accummulates with increasing MMC level and increasing parallel connection, is accounted for by the model.

It is helpful to first examine the general trends in efficiency, power quality and EMI of 2-level and MMC inverters.

2-level converters

Power quality can only be improved by increasing the switching frequency, which degrades efficiency and EMI. High switching frequency increases switching loss and requires fast devices, leading to high EMI [4]. Improvements in efficiency by connecting devices in parallel cannot be realised when switching frequency increases (due to parasitic reactances and skin effect), whilst switch timing errors increase when many devices are connected in parallel at high switching frequency. High switching loss in IGBTs forces the use of switching frequencies below 20kHz [5], leading to poor output waveform quality. SiC MOSFETs support 2-level converters at 1kV, but with reduced switching loss than IGBTs due to near elimination of tail current [6] and comparable on-state conduction loss [7], permitting higher switching frequency and lower EMI.

Modular multilevel converters (MMC)

MMC [8] have already been successfully employed in HVDC scale IGBT inverters resulting in significant reduction in conversion losses over comparable 2 level inverters [9]. A similar approach may be applied to LV (1kVdc) where the low cell voltage facilitates the use of low-voltage Si MOSFETs.

With low cell voltage, low R_{ds_on} MOSFETs may be selected such that the conduction losses do not exceed that of a two level IGBT converter [3].

MMC achieve excellent power quality with low device switching frequency [2,3]. With MMC of around 11-levels or more, switching loss becomes totally insignificant [3]. Low device switching frequency maximizes the efficacy of connecting many devices in parallel to reduce conduction loss, whilst realizing accurate switch timing. With low device switching frequency, and negligible switching losses, device voltage and current transients can afford to slow considerably without degrading converter efficiency. Slow transients should significantly improve EMI [10]. Low MMC cell voltage also reduces EMI, due to reduced ringing amplitude. The MMC further eliminates the need for a bulky, lossy output filter as a result of better waveform quality [11].

Choosing the three highest efficiency devices to represent SiC MOSFET, Si MOSFET and IGBT for comparison with one another was a partly iterative process. The inverter level in which the device is used dictates which device achieves maximum efficiency. For example: in an 11-level MMC, an IGBT with high switching loss, and low conduction loss is more efficient than an IGBT with low switching loss and high conduction loss, however if the same two IGBTs are compared in a 2-level converter then the IGBT with lower switching loss will prove optimal. Therefore, in this paper, the combination of IGBT choice and inverter level which achieves the highest efficiency is used to represent IGBT's in the comparison. A similar iterative process was carried out to choose the inverter level and commerical device for SiC and Si MOSFETs.

EMI can also be improved through careful control of circuit parasitics or choosing diodes with good reverse recovery characteristic. SiC diodes offer improved diode reverse recovery characteristic compared with either IGBT or Si MOSFET technology, while the introduction of Si MOSFETs to converters risks higher EMI due to their faster switching transients and poorer reverse recovery [12]. The detrimental effects of Si MOSFETs on EMI can perhaps be mitigated by slowing switching transitions. Experiments reported below suggest that dramatic EMI reductions can be realized by slowing gate rise- and fall-time.

II. Modelling LVDC Inverter Configurations

LVDC inverters operating from $1kV_{dc}$ link voltage, and delivering 10kW, at $415V_{ac}$ 3-phase will be considered in this analysis. Switching frequency for the 2-level converter is set to 10kHz, with device switching frequency of $10/n$kHz in the MMC, where n is the number of levels in the MMC.

The output voltage and load current on phase **a** is given, as a function of time, t, and mains frequency $\omega=2\pi f$

$$v_a(\omega t) = V_a \sin(\omega t) \tag{1}$$

$$i_a(\omega t) = I_a \sin(\omega t - \varphi) \tag{2}$$

in which $\cos\varphi$ is the power factor. Junction temperature is set to 125°C for all calculations, and it is assumed that heatsinking is sized accordingly. Calculations for all circuit configurations assume that gate voltage conditions are set for minimum on-state losses.

A. IGBT 3-level Converter

With $1kV_{dc}$ input voltage, a 3-level IGBT converter with a 1.2kV IGBT (Infineon IKW40N120H3 [13]) offers lower loss than a 2-level converter with a 1.7kV rated IGBT. The circuit is shown in Fig. 1.

Conduction losses in the devices are found from [14]:

$$P_{cond\_Sm1} = \frac{1}{2\pi}\int_{\alpha}^{\beta}\left[d_{Ta1}(\omega t)i_{a1}(\omega t)\left(V_{ce0}(T_j)+R_{on}(T_j)\right)i_{a1}(\omega t)\right]d(\omega t) \tag{3}$$

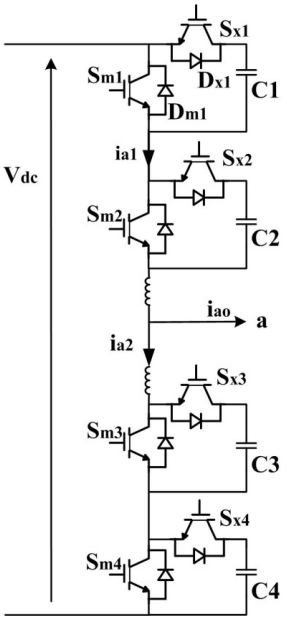

Fig. 1 3-level converter using IGBTs

$$P_{cond\_Dm1} = \frac{1}{2\pi}\int_{\beta}^{\alpha+2\pi}\left[d_{Da1}(\omega t)i_{a1}(\omega t)\left(-V_{f0}(T_j)+R_{on\_D}(T_j)\right)i_{a1}(\omega t)\right]d(\omega t) \tag{4}$$

$$P_{cond\_Sx1} = \frac{1}{2\pi}\int_{\beta}^{\alpha+2\pi}\left[d_{Ta2}(\omega t)i_{a1}(\omega t)\left(-V_{ce0}(T_j)+R_{on}(T_j)\right)i_{a1}(\omega t)\right]d(\omega t) \tag{5}$$

$$P_{cond\_Dx1} = \frac{1}{2\pi}\int_{\alpha}^{\beta}\left[d_{Da2}(\omega t)i_{a1}(\omega t)\left(V_{f0}(T_j)+R_{on\_D}(T_j)\right)i_{a1}(\omega t)\right]d(\omega t) \tag{6}$$

in which V_{ce0} is the IGBT collector-emitter voltage under zero current conditions, $R_{on}(T_j)$ is the incremental on-state resistance of the IGBT, $V_0(T_j)$ is the diode collector-emitter voltage under zero current conditions, $R_{on\_D}(T_j)$ is the incremental on-state resistance of the diode. All parameters are linearly interpolated as a function of junction temperature using figures provided by the manufacturer at 25°C and 175°C, for currents in the range $15\text{-}50A_{rms}$.

Switching losses are found using a curve fit for turn-on and turn-off losses (E_{on} and E_{off} respectively) given in the data sheet, as a function of collector-emitter current, at 175°C, given by (7) and (8). Variation with junction temperature is linearly interpolated between values given for 25°Cand 175°C, which is seen to be a reasonable approximation from Fig. 15 of [13].

$$E_{on} = E_{on\_offset} + [i_a(\omega t)]^2 E_{on\_slope} \tag{7}$$

$$E_{off} = i_a(\omega t) E_{off\_slope} \tag{8}$$

$$P_{sw\_IGBT\_175\deg} = \frac{f_s V_{dc}}{V_{ref} \pi} \int_0^{\pi} \begin{bmatrix} E_{on\_offset} + [I_a \sin(\omega t - \varphi)]^2 E_{on\_slope} \\ + I_a E_{off\_slope} \sin(\omega t - \varphi) \end{bmatrix} d(\omega t) \tag{9}$$

in which E_{on_offset}, E_{on_slope} and E_{off_slope} are constants used in curve-fitting of switching energy as a function of drain current, V_{dc} is the dc link voltage, V_{ref} is the supply voltage at which datasheet switching loss was measured, and f_s is switching frequency. Switching loss at junction temperature T_j is then found from

$$P_{sw\_Tj\_IGBT} = P_{sw\_IGBT\_175\deg} \left[1 - slope(175 - T_j)\right] \tag{10}$$

in which *slope* is the slope of total switching loss as a function of junction temperature T_j.

B. SiC 2-level Converter

The device used for this loss calculation is the 1.7kV Cree CAS300M17BM2 [15], with 16mΩ on-state resistance. The SiC MOSFET 2-level converter, shown in Fig. 2, can also benefit from synchronous rectification, hence loss calculations assume that the diodes do not contribute to the conduction loss, and that the MOSFETs are conducting over the complete cycle. This assumption has been shown to be valid previously by the authors [3]. Conduction loss for one MOSFET is found from:

$$P_{cond\_SiC\_MOS} = \frac{1}{2\pi} \int_0^{2\pi} \left[[i_a(\omega t)]^2 R_{ds\_on}(T_j) \right] d(\omega t) \tag{11}$$

Switching energy is approximately linearly related, through constants K_1 and K_2 to MOSFET drain current as

$$E_{tot} = K_1 + K_2 i_a(\omega t) \tag{12}$$

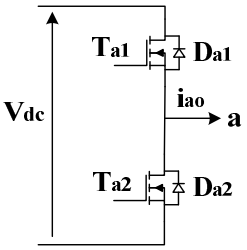

Fig. 2 2-level converter using SiC MOSFETs

However, in synchronous rectification mode, a single switching cycle involves two turn-on and turn-off cycles, due to the fact that the diode conducts briefly during the dead time. The switching steps are listed for commutation between the lower and the upper devices, for the case where the load current is negative:

- At the start T_{a2} is conducting
- T_{a2} turns off and D_{a1} turns on briefly during the dead time
- T_{a1} turns on and D_{a1} turns off
- T_{a1} turns off and D_{a1} turns on briefly during the dead time
- T_{a2} turns back on again and D_{a1} turns off, and one switching cycle is complete.

Switching energy is then adjusted to allow for a lower gate resistance than that used in the data sheet by multiplying by a factor, K_{RG}, calculated from switching energy as a function of gate resistance at a drain current of 300A. Temperature effects on switching loss are seen to be sufficiently small to reasonably be neglected [15].

$$E_{SiC} = \frac{V_{dc} K_{RG}}{V_{ref}} \left[K_1 + \frac{K_2}{\pi} \int_0^{\pi} [I_a \sin(\omega t - \varphi)] d(\omega t) \right] \tag{13}$$

$$P_{sw\_SiC} = 2 f_s E_{SiC} \tag{14}$$

Losses in the SiC 2-level converter at a switching frequency of 10kHz are dominated by switching loss, and so losses for 3-level SiC MMC were calculated, using a lower voltage rated device. However, switching loss in SiC devices does not reduce sufficiently with smaller voltage rating [15], so loss is greater for the 3-level MMC compared with the 2-level.

C. Si MOSFET Modular Multilevel Converter (MMC)

MOSFET voltage rating is chosen to allow for overshoot voltage up to around 170%, using overshoot measurements observed by the authors [3]. The topology of a 3-level MMC converter is shown in Fig. 3. The number of cells in each arm is given by n for a converter with $n+1$ levels. The Si MOSFET MMC calculations have been performed assuming that all operation is in synchronous rectification mode. Hence conduction loss for one cell, P_{cond_cell}, is given by (11). Switching loss must be doubled for synchronous rectification, as discussed for the SiC converter. Switching loss must be estimated separately for the MOSFET and diode as switching energy is not generally given in Si MOSFET datasheets.

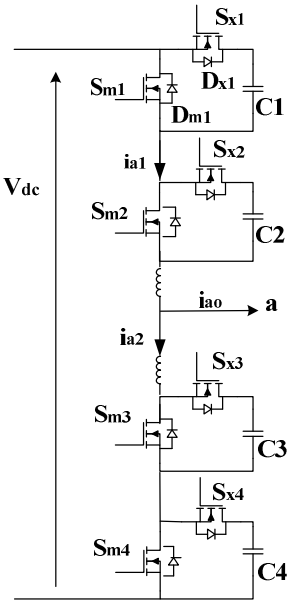

Fig. 3 3-level converter using Si MOSFETs

Referring to Fig. 3, the current in one arm of phase **a** of an MMC converter is given by

$$i_{a1}(\omega t) = I_{dc} + \frac{1}{2} i_a(\omega t) \tag{15}$$

in which I_{dc} is the proportion of dc input current corresponding to phase **a**

MMC MOSFET switching loss is approximated by

$$P_{sw\_MOS\_cell} = \frac{f_s V_{dc}^{\ 2} Q_{sw}}{\pi I_G V_{test} I_{test}} \int_0^{2\pi} [I_{dc} + \frac{1}{2} I_a \sin(\omega t - \varphi)]^2 d(\omega t) \quad (16)$$

in which V_{test} and I_{test} are the voltage and current at which the gate charges are specified in the datasheet. Q_{sw} is the total gate switching charge[16] given by

$$Q_{sw} = \frac{Q_{gs}(V_{gp} - V_{th})}{V_{gp}} + Q_{gd} \quad (17)$$

in which Q_{gs} and Q_{gd} are gate-source and gate-drain charge respectively, V_{gp} is gate-source plateau voltage and V_{th} is threshold voltage. I_G is the average gate voltage during the period from threshold to the end of the Miller plateau (18)

$$I_G = \frac{V_{gg} - V_{gp}}{R_G + R_g} \quad (18)$$

in which R_G is external gate resistance, R_g is internal gate resistance, V_{gg} is the gate drive voltage and V_{gp} is the gate-source voltage during the Miller plateau. The diode switching loss is approximated from reverse recovery charge

$$P_{sw\_diode\_cell} = \frac{2 f_s Q_{rr}(T_j) V_{dc}^{\ 2}}{I_f V_r \pi} \int_0^{\pi} [I_{dc} + \frac{1}{2} I_a \sin(\omega t - \varphi)] d(\omega t) \quad (19)$$

in which $Q_{rr}(T_j)$ is the reverse recovery charge, and V_r and I_f are the reverse voltage and forward current at which $Q_{rr}(T_j)$ was measured.

D. Si MOSFET MMC and SiC 2-level with Parallel-connected Devices

Loss calculations are then performed for Si and SiC MOSFETs operating in synchronous rectification mode, with multiple devices connected in parallel. Formulae used in Section *C* can be modified for connecting *k* devices in parallel by dividing R_{ds_on} by *k* in (11). However, when attempting to use multiple MOSFETs connected in parallel, particularly for the very low voltage rating devices, parasitic track resistance and solder joints will start to become more significant than the R_{ds_on} of the MOSFETs. Measures can be taken to minimize track resistance, but realistic parasitic resistance is likely to reach an order of at least 0.2mΩ at each end to connect to the bus connections joining the cells, and perhaps 0.1mΩ to connect from the bus to each source and drain. Total on-state resistance for the combined devices can therefore be estimated from

$$R_{ds\_comb} = 0.4 + \frac{1}{k}\left(R_{ds\_on} + 0.2\right)\text{m}\Omega \quad (20)$$

Current in each device is now given by

$$i_{device}(\omega t) = \frac{1}{k}\left[I_{dc} + \frac{1}{2} I_a \sin(\omega t - \varphi) \right] \quad (21)$$

MOSFET and diode switching losses for one Si MMC cell therefore become

$$P_{sw\_MOS\_cell\_pal} = k \frac{f_s V_{dc}^{\ 2} Q_{sw}}{\pi I_G V_{test} I_{test}} \int_0^{2\pi} \frac{1}{k^2} [I_{dc} + \frac{1}{2} I_a \sin(\omega t - \varphi)]^2 d(\omega t) \quad (22)$$

$$P_{sw\_diode\_cell\_pl} = k \frac{2 f_s Q_{rr} V_{dc}^{\ 2}}{I_f V_r \pi} \int_0^{\pi} \frac{1}{k} [I_{dc} + \frac{1}{2} I_a \sin(\omega t - \varphi)] d(\omega t) \quad (23)$$

SiC MOSFETs switching loss is not expected to change with parallel-connected SiC devices.

III. Modelled Loss Comparisons

A. Comparing all Technologies with no Parallel Connection

Loss is presented for a range of different levels of MMC, 3-level IGBT, and for 2-level SiC MOSFET. Fig. 4 shows results obtained without using any parallel connection. Table 1 lists the devices used for each configuration.

Table 1 Devices used for loss calculations

Topology	Manufacturer/model	V_{max} (V)	$R_{ds}(on)$ (mΩ)
IBGT 3 level	Infineon IKW40N120H3	1200	18.8
SiC 2 level	Cree CAS300M17BM2	1700	8
Si MMC 7 level	IR IRFP4868	300	25.5
Si MMC 11 level	IR IRFP4668	200	8
Si MMC 17 level	IR IRFP4468	100	2
Si MMC 29 level	Infineon IPT007N06N	60	0.75
Si MMC 43 level	IR IRL7472l1	40	0.34

DC link voltage, V_{dc}, is 1kV throughout, and load current is varied to sweep output power (1 phase) from 0.85 to 10kW. Power factor and modulation index are set to 1, R_G is 1Ω. All devices are chosen to ensure overvoltage does not take place during switching overshoot. At MMC levels lower than 7 switching loss is a fairly significant portion of loss [3]. As MMC level is raised above 17 the reduction in cell voltage is no longer significant to drop to the next MOSFET voltage rating until a level of around 29.

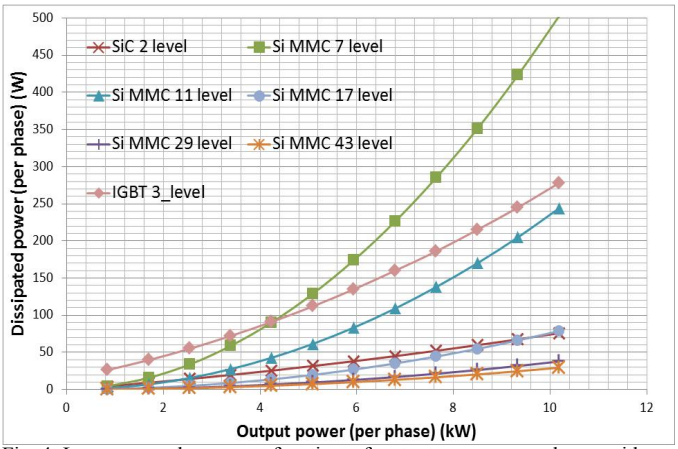

Fig. 4 Losses per phase as a function of output power per phase, with no parallel connection

Examining Fig. 4 it can be seen that IGBT losses rise more gradually with rising load current than MMC topologies. This is because the IGBT losses are dominated by on losses caused by V_{ce0}, which rise as a function of $i_a(\omega t)$, where MMC losses, determined mainly by on-state resistance loss, are proportional to $[i_a(\omega t)]^2$. SiC losses rise very slowly with power because SiC loss comes mostly from switching which rises relatively slowly with increasing current [15]. Consequently, for the Si MMC configurations, above 4kW/phase output power there must be at least 11 levels to exceed IGBT 3-level performance. At least 17 levels are required for Si MMC loss to be lower than SiC, but by 10kW/phase the advantage is turning back to

SiC. Further increases in MMC level achieves the lowest loss, but at very high cost in complexity.

B. Comparing all technologies with parallel connection

The number of devices connected in parallel is varied from 1 to 12, and total losses per phase are calculated, with V_{dc}=1kV and $P_{out/phase}$=3kW, shown in Fig. 5. Parallel-connected device loss is calculated for all the MMC levels, and for the SiC 2-level. Loss is quite dramatically lowered with just 2 parallel-connected devices at the lower levels of Si MMC. This offers a reduction in circuit complexity, volume and weight as 2 parallel-connected devices require simpler control than higher levels of MMC. Improvements obtained by more than 2 devices connected in parallel become less significant as level number increases. For 29- and 43- level MMC, parallel connection actually worsens loss compared to a lower level MMC using the same number of devices connected in parallel (due to the increasing parasitic losses). For SiC, parallel connection has little impact on loss.

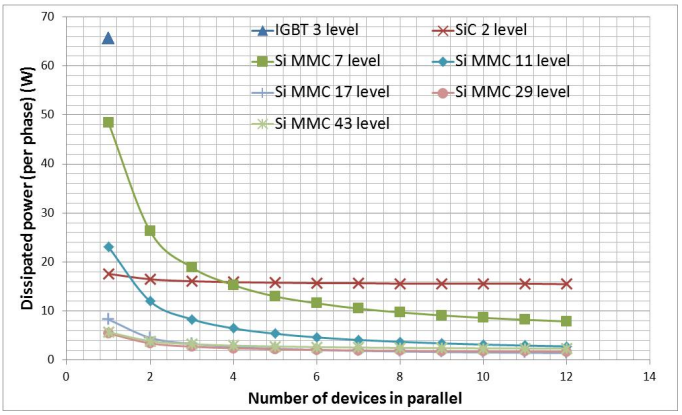

Fig. 5 Losses per phase as a function of the number of MOSFETs connected in parallel. P_{out} per phase = 3kW.

IV. Experimental Validation of Si MMC Loss

Two sets of loss measurements were taken using a 2-level converter with the IR IRFB4127 [17] driven as a 'chopper' at a duty cycle of 50% (a) not in synchronous rectification mode, and (b) in synchronous rectification mode. Measured and calculated results are shown to agree very closely in Fig. 6.

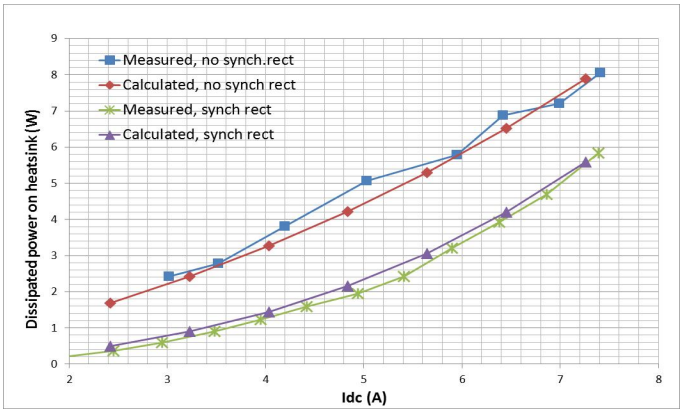

Fig. 6 Loss dissipated in heatsink for chopper operating with and without synchronous rectification

For both (a) and (b), total track resistance was calculated for the PCB, which was not insignificant. Since not all of the heat dissipated in the tracks would act to raise heatsink temperature (some would be radiated), only half of the calculated parasitic resistance was included in the calculation.

V. Implications of MOSFET MMC for EMC

With MMC at higher levels switching loss has been shown to be negligible [3], meaning that an increase in switching loss would not degrade efficiency, allowing slowed switching. In this experiment gate resistance was varied to investigate the relationship between gate-source turn on and diode recovery profile, using the chopper circuit from Section *IV*. Results are presented for MOSFET drain current in Fig. 7 during MOSFET turn on, and MOSFET drain-source voltage in Fig. 8 during turn off, for external gate resistances, R_G, of 5.5–220 Ω.

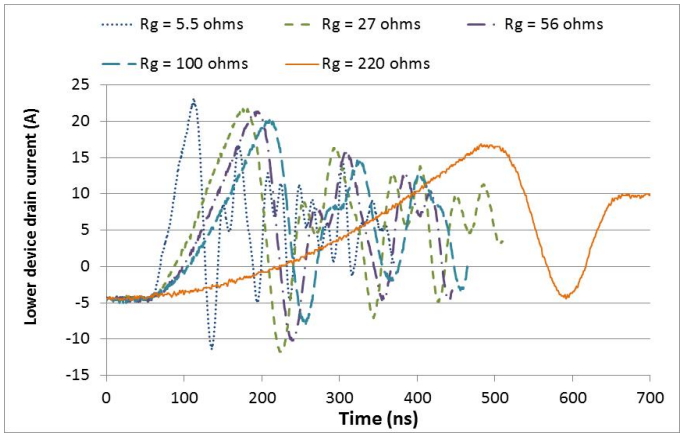

Fig. 7 MOSFET turn on, drain current vs. R_G.

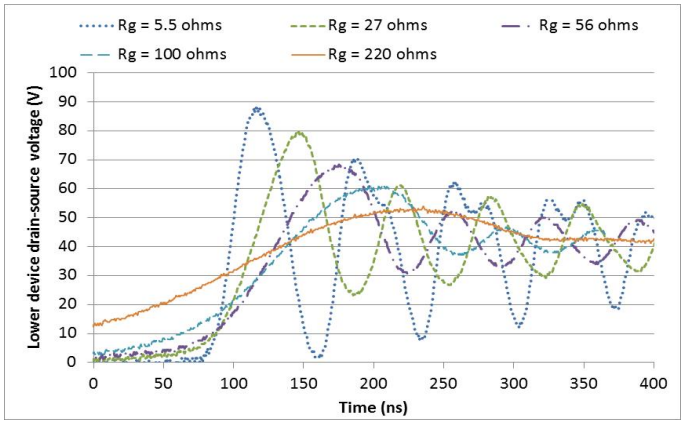

Fig. 8 MOSFET turn off, drain-source voltage vs R_G.

As R_G is increased, both peak reverse recovery current, I_{RRM}, and ringing gradually reduce during MOSFET turn on. It is noticeable that this effect is smaller than the reduction in over-voltage at turn off. Current ringing amplitude has reduced by a factor of approximately 0.85 due to lower rate of change of forward diode current, di_f/dt, and maximum di_f/dt is lower by a factor of approximately 0.158, which is empirically found to be approximately equal to $\sqrt{(R_{G\_old}/R_{G\_new})}$.

Electric fields (*E*-fields) are generated through both differential and common-mode currents, with common-mode

currents tending to dominate EMI radiation [18]. *E*-fields from common mode currents are proportional to both frequency and current magnitude, while *E*-fields from differential mode currents are proportional to the square of frequency [19]. The frequency of interest here is not the switching frequency, but the RF frequencies contained within the spectrum of the fast switching transients, therefore, slowing the switching transient, thus reducing the peak current and the ringing frequency all act to reduce radiated emissions [19]. The relationship between radiated *E*-fields caused by current, frequency content (f) and current amplitude (I_{pk}) are summarized by (24-27).

$$f \propto di_f/dt \propto \sqrt{R_{G\_old}/R_{G\_new}} \tag{24}$$

$$I_{RRM} = I_{pk} \tag{25}$$

$$E_{common\_mode} \propto 20\log\left[fI_{pk}\right] \tag{26}$$

$$E_{differential\_mode} \propto 20\log\left[f^2 I_{pk}\right] \tag{27}$$

The effect on di_f/dt and I_{RRM} at higher current levels is estimated using (24-27), when R_G is increased from 1Ω to 220Ω in the model used in Section *III C*. This change in R_G is calculated to reduce di_f/dt (and therefore frequency) by $\sqrt{(1/220)}$. This reduced di_f/dt can then be used in the datasheet plot of di_f/dt versus I_{RRM} to find that the corresponding reduction in I_{RRM} (and therefore ringing amplitude) is a factor of at least 4. Radiation is therefore estimated to drop by approximately $0.25\sqrt{(1/220)}=35dB$ in common mode and by $0.25[\sqrt{(1/220)}]^2)=59dB$ for differential mode. Despite this much slower switching speed, total calculated loss does not increase for 11-levels and above.

VI. Conclusion

The MOSFET based MMC approach has been shown to produce significantly reduced loss compared with IGBT solutions. The advantage is not so clear between SiC and Si MOSFET MMC. SiC appears to achieve high efficiency with the simplicity of a 2-level converter and promises to achieve low levels of EMI due to good diode reverse recovery profile. Si MOSFET MMC with at least 2 devices connected in parallel and ≥ 11 or more levels promises lower loss than IGBT or SiC in a 10kW 3-phase DC-AC converter. The accuracy of Si MOSFET loss calculations is demonstrated through comparisons of calculated and experimental loss for a single MMC cell, operated as a chopper circuit. This also serves to demonstrate the accuracy of comprehensive estimated parasitic interconnection losses in all the models used in this study. EMI could prove problematic for Si MOSFET MMC compared with SiC. However, experimental results have been presented here showing that slowing of the switching transition using the gate drive can reduce ringing and voltage overshoot, leading to anticipated reduction in radiated electric field of as much as 35-59dB, with no impact on loss.

Acknowledgment

The authors gratefully acknowledge the support of Charles Croser in constructing test circuits, and the financial support of the EPSRC and the NSFC (Joint UK-China research projects on Smart Grids and the Integration of Electric Vehicles), and the EPSRC (www.epsrc.ac.uk, Grant No. EP/I031707/1).

References

[1] A. Emhemed and G. Burt, "The effectiveness of using IEC61660 for characterising short-circuit currents of future low voltage DC distribution networks," in Electricity Distribution (CIRED 2013), 22nd International Conference and Exhibition on, 2013, pp. 1-4.

[2] Y. Zhong, S. Finney and D. Holliday, "An investigation of high efficiency dc-ac converters for LVDC distribution networks", 7th IET International Conference on Power Electronics, Machines and Drives (PEMD 2014), April 2014, pp. 1-6.

[3] Y. Zhong, D. Holliday and S.J. Finney, "Efficiency of MOSFET-based MMC for LVDC distribution systems", IEEE Energy Conversion Congress and Expo (ECCE) 2015, in press.

[4] W. Xuesong, Z. Zhengming and Y. Liqiang, "Conducted EMI reduction in IGBT-based converters", 2010 Asia-Pacific Symposium on Electromagnetic Compatibility (APEMC), April 2010, pp. 230-234.

[5] "IGBTs Or MOSFETs: Which is better for your design?", Electronic Design, Oct 4, 1999, Available here http://electronicdesign.com/interconnects/igbts-or-mosfets-which-better-your-design

[6] A. Anthon, J.C. Hernandez, Z. Zhang and M.A.E. Andersen, "Switching investigations on a SiC MOSFET in a TO-247 package", Proc. of IECON 2014, pp. 1854-1860.

[7] http://www.cree.com/Power/Products/MOSFETs, accessed March 2015.

[8] Q. Tu, Z. Xu and L. Xu, "Reduced switching-frequency modulation and circulating current suppression for modular multilevel converters", IEEE Trans. On Power Delivery, Vol. 26, Issue 3, April 2011, pp. 2009-2017.

[9] Y. Zhang, G.P. Adam, T.C. Lim, S.J. Finney and B.W. Williams, "Voltage source converter in high voltage applications: multilevel versus two-level converters", Proceedings of the 9th IET International Conference on AC and DC Power Transmission 2010, pp. 189-193.

[10] X. Zhu, D. Su, Y. Zhang and l. Wei, "Bus bar design for EMC performance of power converters in fuel cell electric vehicles", IEEE International Conference on Vehicular Electronics and Safety, Dec 2006, pp. 144-147.

[11] W. li, L.A. Gregoire and J. Belanger, "Control and performance of a modular multilevel converter system", Cigre Canada, Conference on Power Systems Sep 2011.

[12] M. Liang, T.Q. Zheng and Y. Li, "Performance evaluation of SiC MOSFET, Si CoolMOS and IGBT", 2014 International Electronics and Application Conference and Exposiation (PEAC), Nov 2014, pp. 1369-1373.

[13] Infineon IKW40N120H3, available at www.infineon.com, accessed March 2015.

[14] K. Berringer, J. Marvin and P. Perruchoud, "Semiconductor power losses in AC inverters", IEEE Industry Applications Conference, 1995, Vol. 1, pp. 882-888.

[15] CAS300M17BM2 from Cree, available at http://www.cree.com, accessed March 2015.

[16] ON Semiconductor Application Note AND9083/D "MOSFET gate-charge origin and its applications", available at http://onsemi.com, accessed March 2015.

[17] IRFB4127 MOSFET from International Rectifier, data sheets available at http://www.irf.com/part/_/A~IRFB4127, accessed March 2015.

[18] Mark I. Montrose, EMC and the printed circuit board, Wiley IEEE press, ISBN: 978-0-7803-4703-8, 1998, pp.

[19] Module 9, "Radiated emissions", EM Research group, Michigan State University, notes compiled under the NSF founded GOALI program. Available at http://www.egr.msu.edu/em/research/goali/notes/module9_radiated_emissions.pdf, accessed March 2015.